Theor. Appl. Climatol. 71, 17–28 (2002)

Theoretical and Applied Climatology

[1] Department of Geography, University of Haifa, Haifa, Israel
[2] Israel Meteorological Service, Israel

North Sea-Caspian Pattern (*NCP*) – an upper level atmospheric teleconnection affecting the Eastern Mediterranean: Identification and definition

H. Kutiel[1] and **Y. Benaroch**[1,2]

With 6 Figures

Received March 8, 2001
Revised July 3, 2001

Summary

An upper level atmospheric teleconnection between grid points: 0°, 55° N; 10° E, 55° N (North Sea) and 50° E, 45° N; 60° E, 45° N (northern Caspian) was identified. This teleconnection, referred as the *North Sea-Caspian Pattern* (*NCP*) is evident at the 500 hPa level. The *NCP* is more pronounced during winter and the transitional seasons. An index (*NCPI*) measures the geopotential heights differences between the two poles of the *NCP*. Time series of the *NCPI* are presented and analysed. Except for September, no significant temporal trends were found. Negative and positive phases of the *NCP* (*NCP*(−) and *NCP*(+), respectively) were defined using standardized scores. A classification of all months into *NCP*(−), *NCP*(+) or normal conditions during the analysis period (1958–1998) was prepared and analysed. No significant correlation was found between the *NCPI* and the *NAO* index. The anomalous circulation during either *NCP*(−) or *NCP*(+) conditions is defined and its possible impact on the regional climate is discussed. Preliminary results show below normal temperatures and above normal precipitation in the Balkans and the Middle East during *NCP*(+), and the opposite for *NCP*(−).

1. Introduction

Atmospheric teleconnections on global or regional scales and their influence on temperature and precipitation regimes have been studied widely. Certainly, the most widely known teleconnection is the *Southern Oscillation* (*SO*) related to the *El Niño* effect and referred to by the acronym *ENSO*. Many studies relate the *ENSO* with climatic conditions and their resulting economic, societal and environmental effects, throughout the world. Another widely studied teleconnection is the *North Atlantic Oscillation* (*NAO*). This oscillation, between the Azores and Iceland, primarily affects the rainfall regime in northwestern Africa (Morocco) and northwestern Europe (e.g. van Loon and Rogers, 1978; Rogers and van Loon, 1979; Wallace and Gutzler, 1981; Rogers, 1984; Barnston and Livezey, 1987; Lamb and Peppler, 1987; Glowienka-Hense, 1990; Rogers, 1990; Hurrell, 1995; Stephenson et al., 2000). The *NAO* also has an important role in determining the winter characteristics of wider regions in Europe. Other teleconnections have been identified and defined in that region. Kutiel and Kay (1992), defined the *SENA* (*Southern Europe-North Atlantic*) index. Recently, Yin (1999), collected and mapped the centers of action for many teleconnections published in the literature. Some of these teleconnections are at higher levels and not only occur at sea level, e.g. the *Eastern Atlantic pattern* (*EA*) at the 700 hPa level, defined by Esbensen (1984) and the *Scandinavian pattern* (*SCAND*). The role of these teleconnections, however, in influencing

the climate of the Mediterranean in general, and of its eastern basin in particular, has seldom been studied.

Conté et al. (1989), suggested the existence of a so-called *Mediterranean Oscillation*, at the 500 hPa level between the two extremes of the Mediterranean basin. Their suggestion was based on a dipole effect they found between Alger and Cairo in mean annual geopotential heights at the 500 hPa level. They tried to relate this oscillation with precipitation in Italy. Based on the concept of a *Mediterranean Oscillation*, a dipole behaviour of other climatic parameters (temperature, precipitation, circulation, etc.) between the western and eastern Mediterranean were reported and attributed to this oscillation (Kutiel et al., 1996; Maheras et al., 1997, 1998, 1999; Douguédroit, 1998; Kutiel and Maheras, 1998; Kutiel and Paz, 1998; Maheras and Kutiel, 1999).

The purpose of the present study are: (a) to identify and validate the existence of such a teleconnection at the 500 hPa geopotential level, (b) to determine its location, (c) to define an index similar to the *NAO* index or other such indices and to evaluate its magnitude, (d) to calculate a time series of that index. Such a time series may be used to check for long-term changes in the intensity of any teleconnections and can be correlated with other climatic time series to identify possible impacts of the teleconnection.

2. Data and methodology

Mean monthly geopotential heights at the 500 hPa level for 66 grid points on a 10° longitude by 10° latitude grid, in the region delimited by the 30° W and 70° E meridians and 15° N and 65° N parallels, were used. We used *Monthly Intrinsic Pressure Level phi Geopotential height* grided data, for the period 1958–1998, obtained from *NOAA NCEP-NCAR*.

Linear correlations were calculated between mean monthly geopotential heights at each grid point, with all other grid points. A total of 2145 ($66^{*}65/2$) correlations were calculated for each month. As one would expect, correlation coefficients of adjacent grid points showed high positive values, which decreased with increasing distance between grid points. However, as one of the main purposes of this study was to define the location of the poles with a dipole-like behaviour, only the significant *negative* correlations were retained. These were found at greater distances from respective grid points. In each month, each pair of grid points having a significant ($p \leq 0.05$) negative correlation was connected by a line, yielding a map as shown in Fig. 1.

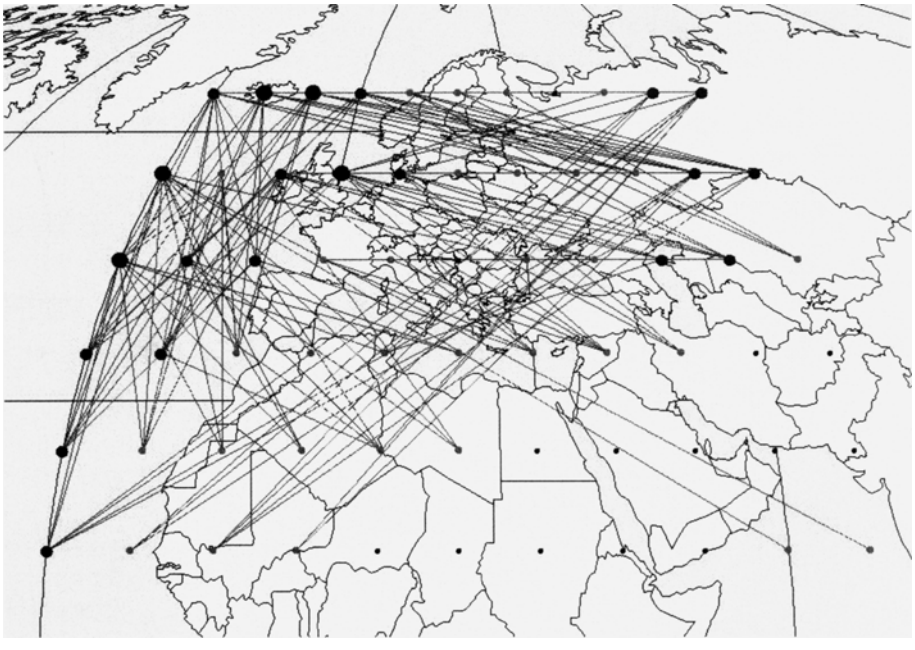

Fig. 1. An example of a monthly map in which every pair of grid points, within the study area, having a significant negative correlation, were connected with a line. Grid points' sizes are relative to the number of significant correlations of that point

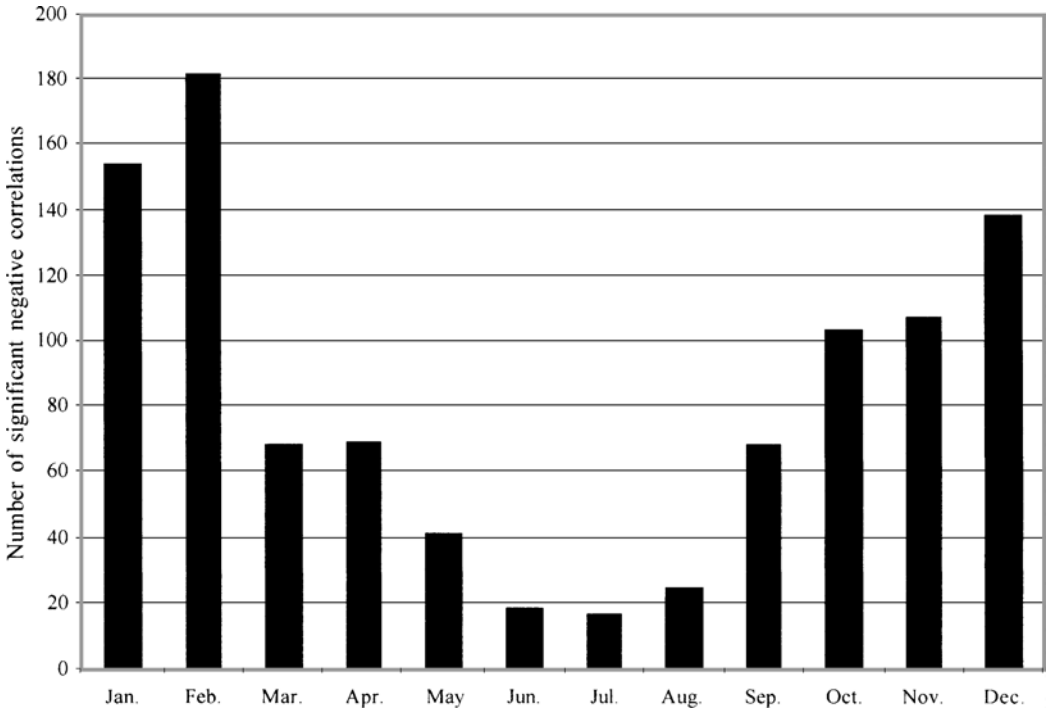

Fig. 2. The annual course of the number of significant negative correlations between pairs of grid points

Figure 2 illustrates the annual pattern of the number of significant negative correlations between pairs of grid points. A clear annual pattern occurs, with large numbers in winter (maximum in February) and a sharp decrease in summer (minimum in July). The maximum number of significant negative correlations accounts for about 7%–8% of the total number of correlations in winter and drops to less than 1% in summer. This implies that the dipole-like behaviour between different locations within the study area is much more pronounced during winter.

A GIS (Arc View) was used to differentiate between the various levels of the significant correlations to enable more accurate location of the poles of the teleconnection. The definition of the teleconnection and its poles was also based on the persistence of the location with a large number of negative correlations all or most of the year round. Using this criterion, we were unable to find a teleconnection across the Mediterranean itself, but a different teleconnection located north of the Mediterranean was identified. Two poles were defined at 0°, 55° N; 10° E, 55° N (North Sea) and 50° E, 45° N; 60° E, 45° N (northern Caspian). It was therefore, named the *North Sea-Caspian Pattern* or *NCP* hereafter. The *NCP* probably reflects the *Euroasia-2 Pattern* (also referred to sometimes as the *East Atlantic/ Western Russia pattern*) defined by Barnston and Livezey, (1987) at the 700 hPa geopotential level. We believe that our name provides a better definition of the geographical extent of this teleconnection.

An index defining the *NCP* intensity was calculated as follows:

$$NCPI = \overline{gpm}(0^\circ, 55^\circ N; 10^\circ E, 55^\circ N) - \overline{gpm}(50^\circ E, 45^\circ N; 60^\circ E, 45^\circ N)$$

where, *gpm* (geo-potential metres) is the average height of the two grid points forming each of the two poles, respectively. This index enabled the calculation of monthly time series of the *NCPI*.

For each month the data were then standardized as follows:

$$z_i = (NCPI_i - \overline{NCPI})/\sigma$$

where, $NCPI_i$ *is the monthly NCPI in the year i*; $\overline{NCPI}$ is the monthly long-term *NCPI* average and σ is its standard deviation.

Table 1, lists the time series of the standardized scores of monthly *NCPI*. It can be seen that

Table 1. Standardized scores (z_i) of monthly *NCPI*

	Jan.	Feb.	Mar.	Apr.	May	Jun.	Jul.	Aug.	Sep.	Oct.	Nov.	Dec.
1958	−0.899	−0.922	−0.615	0.529	−0.888	−0.583	0.077	−0.450	1.603	0.408	1.771	−0.740
1959	−1.371	2.789	1.290	−0.467	0.696	0.946	1.101	2.098	2.251	0.951	0.543	−1.116
1960	−0.484	−1.048	1.282	0.436	1.618	0.574	−0.959	−0.886	0.187	−1.239	−1.382	−1.424
1961	−0.522	0.431	1.777	0.358	−1.251	0.054	−0.237	−0.563	1.955	−0.174	0.659	−0.211
1962	−0.432	0.082	−2.057	0.085	−0.979	0.362	−1.237	−1.455	−0.854	1.234	−0.287	−0.203
1963	−0.394	−1.156	0.697	0.002	0.456	0.271	0.539	−1.027	−0.058	0.167	−0.482	1.000
1964	2.275	0.067	0.179	1.120	0.573	0.396	0.454	0.545	0.206	−0.128	1.321	−0.913
1965	−0.846	0.738	−0.234	0.632	−0.765	−0.069	−1.516	−1.398	−0.517	1.738	−0.849	−1.981
1966	−0.808	−1.075	−0.039	−0.209	0.280	0.520	−0.702	−0.490	0.488	−0.739	−1.904	−1.064
1967	−0.135	0.449	0.043	0.393	−1.345	0.891	1.101	−0.595	0.076	−1.135	0.381	−0.017
1968	0.151	−0.745	0.064	0.032	−1.640	0.780	0.275	0.289	−0.776	0.143	0.537	−0.012
1969	0.498	−0.768	0.175	−0.226	−0.230	−0.188	2.084	−0.109	1.603	2.042	−1.834	−0.155
1970	−0.521	−1.611	−1.817	−2.137	0.730	1.690	−0.705	0.950	0.307	0.158	−0.429	1.005
1971	−1.007	0.946	−0.802	0.786	0.426	−0.505	0.574	0.367	0.095	1.201	−0.344	1.946
1972	0.947	−0.229	0.911	−0.760	−0.671	−1.062	0.936	0.224	0.005	0.563	−0.273	1.341
1973	1.566	−0.509	1.697	−0.609	0.068	1.142	0.179	0.672	0.968	−0.024	−0.048	−0.472
1974	0.751	−0.569	−0.223	2.068	−0.551	−0.381	−0.899	0.698	−1.634	−2.260	−1.039	−0.046
1975	−0.163	1.808	−0.256	−1.527	−0.313	−0.042	0.012	1.664	−0.448	1.074	0.713	1.030
1976	−0.091	1.280	0.326	0.563	−0.170	1.274	1.244	0.107	−0.081	0.259	−0.367	−1.558
1977	−0.076	−1.459	−0.432	−1.845	−0.213	−0.383	−0.032	0.200	0.185	1.017	−1.387	1.190
1978	−0.468	−1.039	−1.347	0.656	1.310	0.029	−1.129	−0.476	−1.242	0.893	1.987	−0.039
1979	−1.395	−0.283	−1.902	−0.396	−1.511	0.824	−0.969	−1.888	−0.532	0.285	−1.340	−0.339
1980	0.219	0.508	−0.485	0.721	−0.221	−1.126	−1.468	0.081	0.878	−0.427	−0.015	−0.699
1981	−0.303	0.250	−0.545	1.591	0.348	0.232	−0.434	1.057	−0.502	−2.380	0.439	−2.207
1982	0.421	1.177	0.303	−0.041	−0.771	−0.039	1.162	−0.547	0.803	−0.028	0.102	−0.704
1983	0.610	−0.031	0.200	−1.271	−1.559	0.826	1.297	1.955	−0.201	−0.156	1.071	0.136
1984	−1.689	0.243	−0.205	1.243	−0.461	−0.540	−0.884	1.037	−2.076	−0.300	0.358	0.915
1985	−0.889	1.049	−0.175	−0.702	−0.141	−1.665	0.109	−1.376	0.125	1.881	−1.348	0.058
1986	−1.357	−0.426	−0.085	−2.108	0.458	1.167	−0.615	−1.767	−0.793	−0.031	0.774	0.230
1987	0.016	−0.398	−0.132	1.806	−1.100	−2.518	−0.008	−0.920	0.000	−0.389	0.337	0.862
1988	−0.545	−1.198	−1.179	−0.072	1.123	0.482	−1.189	−0.662	−0.171	−0.243	1.044	1.091
1989	2.158	0.104	−0.692	−0.829	1.830	−0.175	0.189	−0.708	1.174	−0.089	0.785	0.412
1990	0.472	−0.735	1.206	0.486	1.204	−0.693	0.399	1.146	−1.203	0.011	−0.266	0.370
1991	0.812	−0.257	0.494	−0.344	1.363	−2.495	0.903	0.902	0.385	−0.604	−0.343	2.021
1992	2.244	1.132	0.221	0.049	2.370	1.759	0.418	−0.331	−0.019	−1.225	−0.501	0.956
1993	0.572	1.625	1.447	0.725	1.159	0.427	−1.291	−0.397	−0.757	−0.337	1.642	−1.500
1994	−0.976	0.545	−0.749	−0.538	0.014	0.341	2.353	−0.139	−1.948	−0.875	1.509	0.673
1995	−0.919	−1.264	−1.772	−0.103	−0.587	0.081	1.123	1.594	−1.160	1.093	0.591	0.624
1996	0.356	−0.738	0.634	0.943	−1.236	0.405	−0.928	0.004	0.797	−0.044	−1.623	−0.264
1997	1.591	−0.083	1.808	0.602	−0.175	−1.067	0.258	1.100	1.408	−0.671	−0.162	0.172
1998	0.631	1.319	0.989	−1.640	0.754	−1.945	−1.584	−0.504	−0.527	−1.619	−0.343	−0.366

values are either negative, positive, or close to zero. In order to differentiate between these cases, a threshold value of $|0.5|$ was set. Months were classified in the *Negative phase of NCP* (*NCP*(−) hereafter) when: $z_i \leq -0.5$. Similarly, a month was classified in the *Positive phase of NCP* (*NCP*(+)) when: $z_i \geq +0.5$. Table 2 lists the classification of months according to whether they belong to *NCP*(−) or *NCP*(+). Months belonging to neither *NCP*(−) nor *NCP*(+), were considered normal and left blank in Table 2.

3. Results and discussion

Figure 3 shows the annual cycle of the minimum, average and maximum *NCPI*. On average the *NCPI* is negative all year around. The range between the maximum and minimum *NCPI* is greater in winter and smaller in summer, which

Table 2. Definition of the months as belonging to *NCP*(−) or *NCP*(+)

	Jan.	Feb.	Mar.	Apr.	May	Jun.	Jul.	Aug.	Sep.	Oct.	Nov.	Dec.
1958	N	N	N	P	N	N			P		P	N
1959	N	P	P		P	P	P	P	P	P	P	N
1960		N	P		P	P	N	N		N	N	N
1961	N		P		N			N	P		P	
1962			N		N		N	N	N	P		
1963		N	P				P	N				P
1964	P			P	P			P			P	N
1965	N	P		P	N		N	N	N	P	N	N
1966	N	N				P	N			N	N	N
1967					N	P	P	N		N		
1968		N			N	P			N		P	
1969		N					P		P	P	N	
1970	N	N	N	N	P	P	N	P				P
1971	N	P	N	P		N	P			P		P
1972	P		P	N	N	N	P			P		P
1973	P	N	P	N		P		P	P			
1974	P	N		P	N		N	P	N	N	N	
1975		P		N				P		P	P	P
1976		P		P		P	P					N
1977		N		N						P	N	P
1978		N	N	P	P		N		N	P	P	
1979	N		N		N	P	N	N	N		N	
1980		P		P		N	N		P			N
1981			N	P				P	N	N		N
1982		P			N		P	N	P			N
1983	P			N	N	P	P	P			P	
1984	N			P		N	N	P	N			P
1985	N	P		N		N		N		P	N	
1986	N			N		P	N	N	N		P	
1987				P	N	N		N				P
1988	N	N	N		P		N	N			P	P
1989	P		N	N	P			N	P		P	
1990		N	P		P	N		P	N			
1991	P				P	N	P	P		N		P
1992	P	P			P	P				N	N	P
1993	P	P	P	P	P		N		N		P	N
1994	N	P	N	N			P		N	N	P	P
1995	N	N	N		N		P	P	N	P	P	P
1996		N	P	P	N		N		P		N	
1997	P		P	P		N		P	P	N		
1998	P	P	P	N	P	N	N	N	N	N		

shows that the *NCP* is less evident and has a reduced importance during summer. Table 3 lists the number of years in which the *NCPI* was negative or positive. During the warm period (April–September) the number of positive *NCPI* values was zero or negligible. Positive *NCPI* values were obtained only in transitional months (October, November or March) in 15% of all years, and in winter (December–February) in 30% of all years. This implies that most of the time the pressure over the northern Caspian Sea is higher than pressure over the North Sea, and the circulation is based on this situation. Positive *NCPI* occur only during extreme cases, never in May, June, or August during the study period (Fig. 3 and Table 3). These values shouldn't be confused with the *NCP*(−) or *NCP*(+). It is quite possible that in a month defined as *NCP*(+), the *NCPI* will have a *negative* value.

Figure 4 shows the time series of the standard monthly *NCPI*. The shaded areas on each figure represent the regions defined as *NCP*(−) or

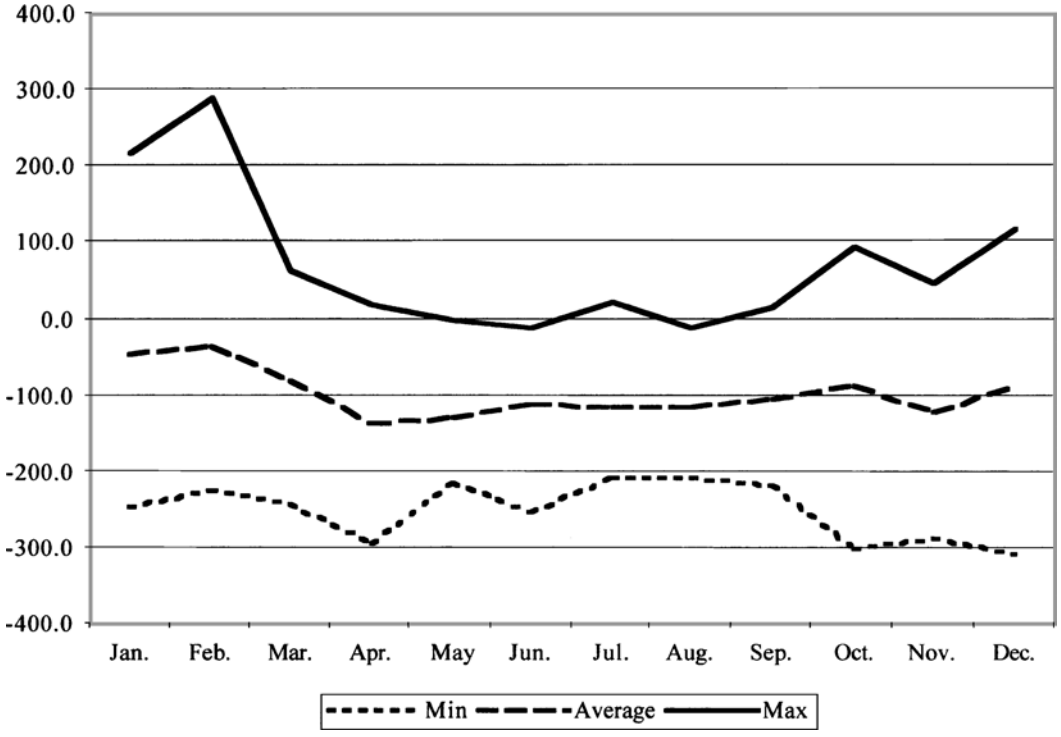

Fig. 3. Annual course of minimum, average and maximum *NCPI*

Table 3. The distribution of negative and positive *NCPI* values in each month

Month	# of years with negative values	# of years with positive values
January	27	14
February	27	14
March	34	7
April	40	1
May	41	–
June	41	–
July	39	2
August	41	–
September	40	1
October	33	8
November	37	4
December	30	11

NCP(+) respectively. The white strip in the middle represents normal cases.

About 30% of all months were defined as *NCP*(−) and a similar number of months as *NCP*(+). The remaining 40% were defined as normal months (Table 2 and Fig. 4). Choosing a different threshold value would have changed the proportions of the cases in each of the phases. Setting a larger threshold value (e.g. $z_i \geq |1.0|$), would have reduced considerably the number of cases belonging to each phase. With such a large threshold only very few extreme cases would belong to each phase, preventing any statistical analysis. Lowering this threshold to for example $z_i \geq |0.25|$, would have classify too many cases either in the negative, or positive phases, which would mask the impact of each phase.

The temporal distribution of both phases was not constant during the year. In the transitional months more *NCP*(+) cases than *NCP*(−) cases occurred, whilst the opposite is true in winter (Fig. 5). Furthermore, *NCP*(−) episodes are more persistent than *NCP*(+) episodes. We identified 14 episodes of *NCP*(−) lasting for at least three consecutive months, but only eight such *NCP*(+) episodes, with four of them occurring during the 1990s (Table 2).

The time series of the *NCPI* demonstrates high interannual variability which increases in recent years, mainly evident in June (Fig. 4). No significant temporal trend was present. September was the only month with a significant negative trend [$p = 0.0423$]. The slope of this trend is -1.4 [gpm/yr]. A decrease of the *NCPI* may result from either a decrease of the geopotential heights over the North Sea, or an increase over the Caspian Sea, or a combination of both

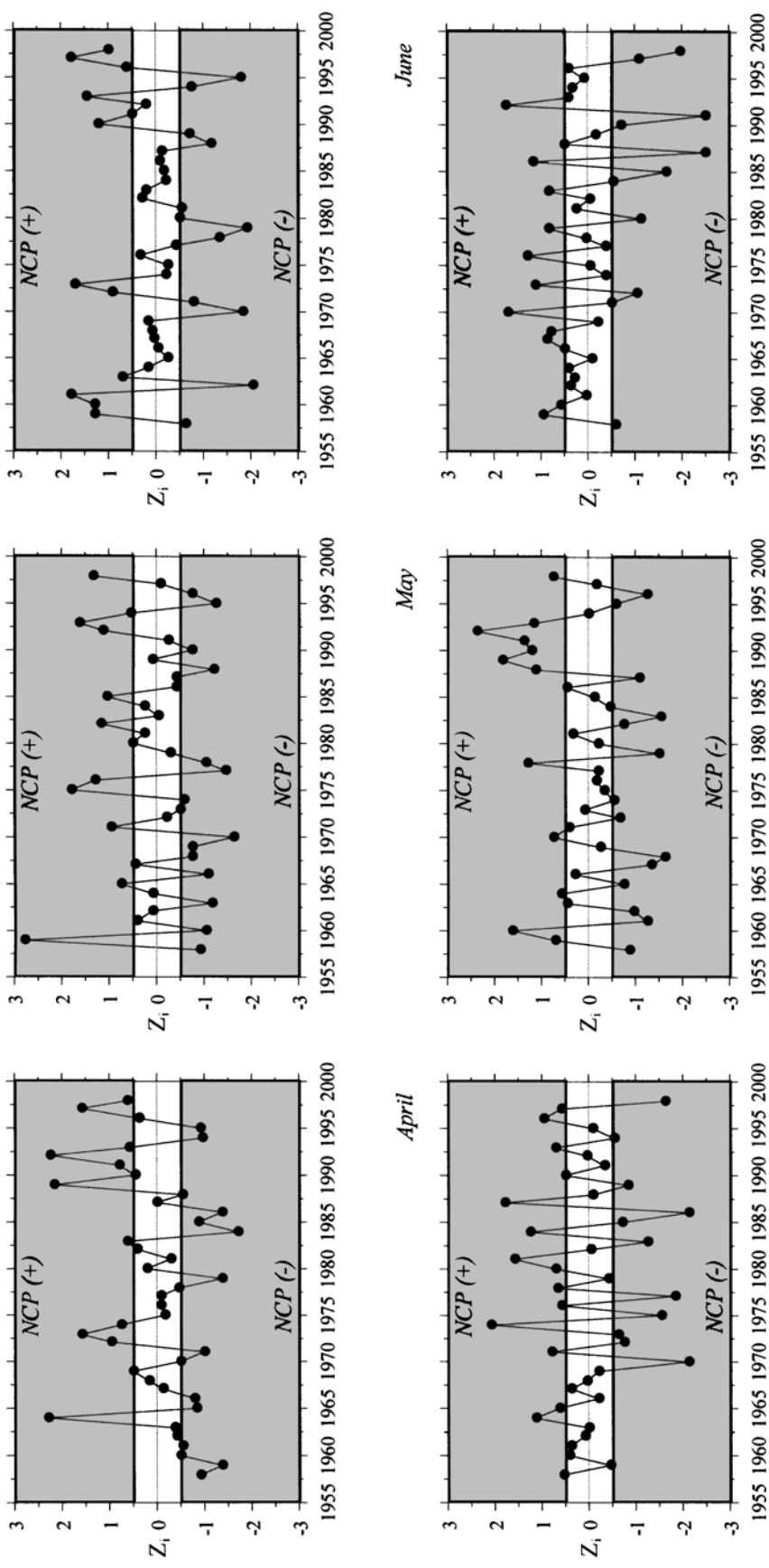

Fig. 4. Time series of standardized monthly *NCPI*. The shaded areas on each figure represent the regions defined as *NCP*(−) or *NCP*(+) respectively, and the white strip in the middle represents the normal cases

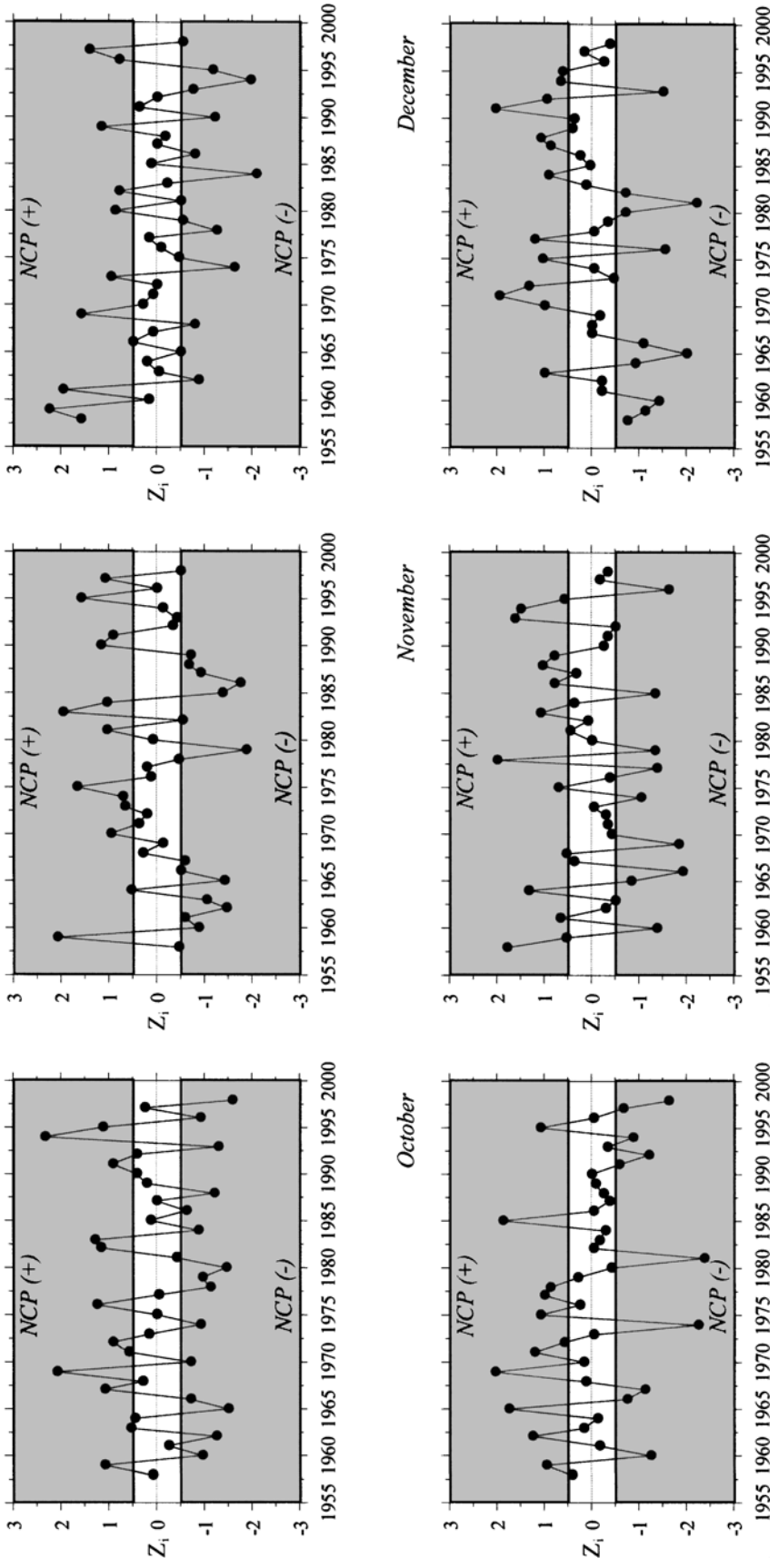

Fig. 4 (continued)

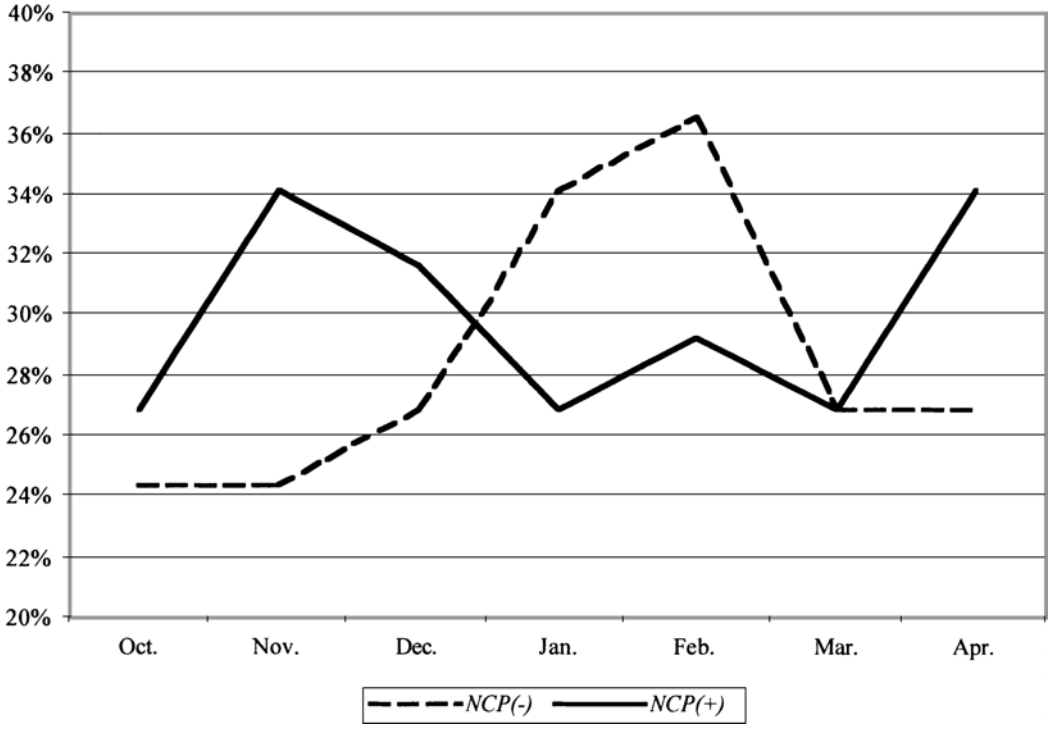

Fig. 5. Seasonal course of the percentage of *NCP*(−) and *NCP*(+) out of all cases (41 years)

these changes. To verify the causes of the decrease in the *NCPI* we calculated temporal trend of the geopotential heights over both poles of the *NCP*. There was no significant trend over the North Sea although a significant increase over the northern Caspian Sea was identified, which we attribute to the decrease in the *NCPI* in September.

Monthly correlations were calculated between *NCPI* and *NAO* indices (defined as the normalized pressure difference between Ponta-Delgada in the Azores and Reykjavik in Iceland) for the study period. All correlation coefficients, apart from one, were positive, but not significant at the 0.05 level (Table 4). The results indicate that both teleconnections behave almost independently and we cannot predict one index based on the behaviour of other.

Table 4. Correlation coefficients between monthly *NCPI* and monthly *NAO* indices (n.s. – not significant at the 0.05 significance level)

Month	Correlation coefficient (r)	p value
January	.202	n.s.
February	.265	n.s.
March	.280	n.s.
April	−.116	n.s.
May	.149	n.s.
June	.221	n.s.
July	.096	n.s.
August	.086	n.s.
September	.163	n.s.
October	.330	.0351
November	.080	n.s.
December	.046	n.s.

An *NCP*(−) implies an *increased counterclockwise* anomaly circulation around the *western* pole of the *NCP* and an *increased clockwise* anomaly circulation around the *eastern* pole of the *NCP* (Fig. 6a). Similarly, during the *NCP*(+), we should expect an *increased clockwise* anomaly circulation around the *western* pole of the *NCP* and an *increased counterclockwise* anomaly circulation around the *eastern* pole of the *NCP* (Fig. 6b).

During the *NCP*(−), these anomalous circulation patterns imply an increased westerly anomaly circulation towards central Europe, and an increased easterly anomaly circulation towards Georgia, Armenia and eastern Turkey. This results in an increased southwesterly anomaly circulation

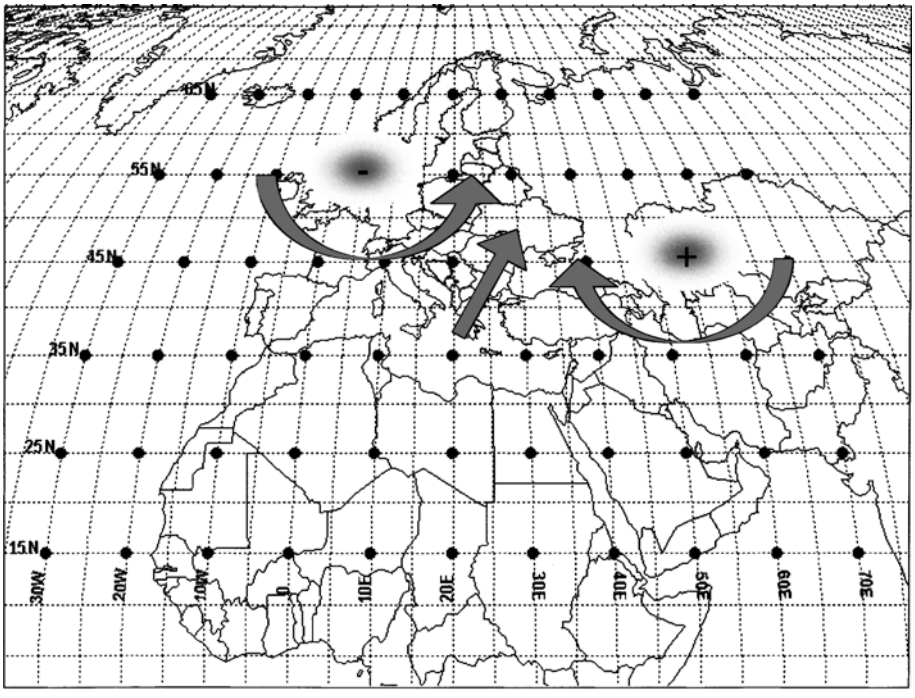

a

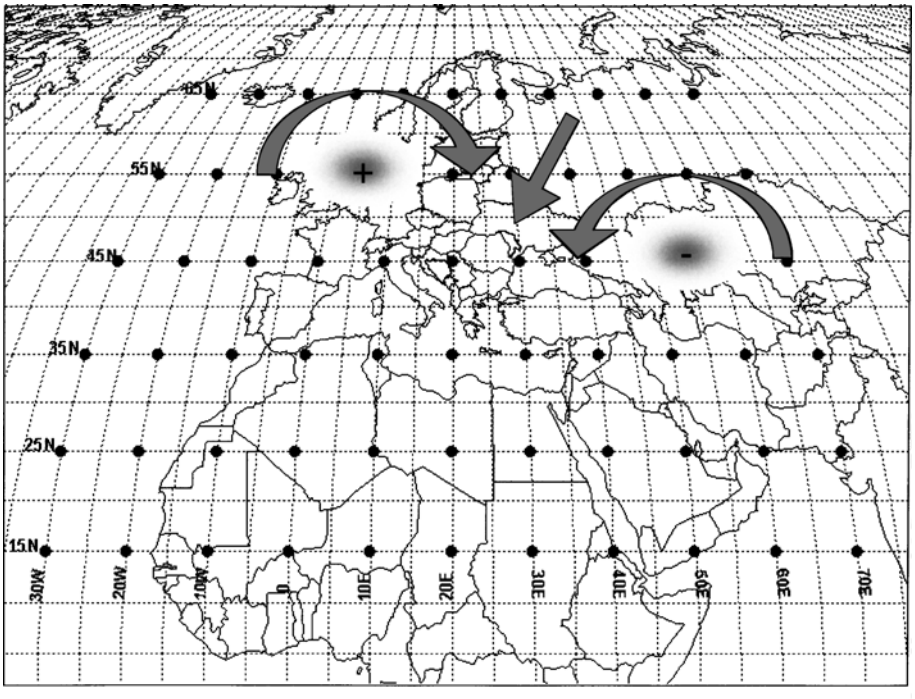

b

Fig. 6. A schematic representation of the anomaly circulation affecting the Mediterranean and surrounding regions during *NCP* (−) (**a**) and *NCP*(+) (**b**) episodes

towards the Balkans and western Turkey. Similarly, during the *NCP*(+), the circulation suggests an increased northwesterly circulation towards eastern Europe, and an increased northeasterly circulation towards the Black Sea. This results in an increased northeasterly anomaly circulation towards the Balkans (Fig. 6a and 6b). Based on the above scheme, one should expect to find the maximum differences between *NCP*(−) and *NCP*(+) to occur over the Balkans and the Middle East. A preliminary analysis of January air temperatures at Athens revealed that the average temperature during *NCP*(−) was 10.1 °C while during *NCP*(+) only 8.2 °C. The average

temperature for all Januarys is 9.3 °C. Similarly, a comparison of monthly rainfall totals at Haifa (northern Israel) reveals that during *NCP*(−) rainfall is below average, only 547 mm, while during *NCP*(+) rainfall is above average, 908 mm. The average rainfall is 703 mm.

Our results therefore do not show a seesaw behaviour in the upper level pressure patterns across the Mediterranean. Thus, we are unable to confirm the presence of the *Mediterranean Oscillation* as suggested by Conté et al. (1989). However, seesaw behaviour across the Mediterranean, has been found in other meteorological variables (e.g. air temperature, precipitation, etc.), in several studies referred to earlier. Thus we may refer to this pattern as an exhibition of the above concept proposed by Conté. In such a case we may attribute it to the existence of the *NCP*, located north of the Mediterranean.

4. Conclusions

We may summarize our main conclusions as follows:

1. Teleconnections within the study area are more frequent in winter (maximum in February) than in summer (minimum in July).
2. A teleconnection was identified between the North Sea and the Caspian at the 500 hPa geopotential level. We refer to this as the *North-sea-Caspian Pattern* or *NCP*.
3. An index (*NCPI*) that measures the intensity of the *NCP* was defined as follows: $NCPI = \overline{gpm}\,(0^\circ, 55^\circ N; 10^\circ E, 55^\circ N) - \overline{gpm}\,(50^\circ E, 45^\circ N; 60^\circ E,\ 45^\circ N)$
4. Most of the year the *NCPI* is negative. The *Negative and Positive phases of NCP* (*NCP* (−) and *NCP*(+) respectively) were defined using standardized scores: *NCP*(−) when: $z_i \leq -0.5$ and *NCP*(+) when: $z_i \geq +0.5$.
5. *NCP*(−) episodes (consecutive months belonging to the same phase) are more frequent than *NCP*(+) episodes. However, during the 1990s, there has been an increase in the frequency of *NCP*(+) episodes.
6. *NCP*(−) episodes tend to bring an increased southwesterly anomaly circulation towards the Balkans, western Turkey and the Middle East, causing above normal temperatures and below normal precipitation in these regions. The opposite occurs with *NCP*(+), episodes.
7. The *NCP* is an example of the *Euroasia*-2 pattern (*East Atlantic/Western Russia* pattern) at the 500 hPa level and is probably partly responsible for dipole behaviour across the Mediterranean, referred to as the *Mediterranean Oscillation*. No significant correlation was found between the *NCPI* and the *NAO* index.

References

Barnston AG, Livezey RE (1987) Classification, seasonality and persistence of low-frequency atmospheric circulation patterns. Mon Wea Rev 115: 1083–1126

Conté M, Giuffrida A, Tedesco S (1989) The Mediterranean oscillation. Impact on precipitation and hydrology in Italy. Conference on: Climate Water. Publications of the Academy of Finland, Helsinki. 11–15 September 1989, 121–137

Douguédroit A (1998) L'oscillation Méditerranéenne: Le cas du printemps. Pub Assoc Int Climatol 11: 383–390

Esbensen SK (1984) A comparison of intermonthly and interannual teleconnections in the 700 mb geopotential height field during the northern hemisphere winter. Mon Wea Rev 112: 2016–2032

Glowienka-Hense R (1990) The north Atlantic oscillation in the Atlantic-European SLP. Tellus 42A: 497–507

Hurrell JW (1995) Decadal trends in the North Atlantic Oscillation: Regional temperatures and precipitation. Science 269: 676–679

Kutiel H, Kay PA (1992) Recent variations in 700 hPa geopotential heights in summer over Europe and the Middle East, and their influence on other meteorological factors. Theor Appl Climatol 46: 99–108

Kutiel H, Maheras P (1998) Variations in the temperature regime across the Mediterranean during the last century and their relationship with circulation indices. Theor Appl Climatol 61: 39–53

Kutiel H, Paz S (1998) Sea level pressure departures in the Mediterranean and their relationship with monthly rainfall conditions in Israel. Theor Appl Climatol 60: 93–109

Kutiel H, Maheras P, Guika S (1996) Circulation indices over the Mediterranean and Europe and their relationship with rainfall conditions across the Mediterranean. Theor Appl Climatol 54: 125–138

Lamb PJ, Peppler RA (1987) North Atlantic oscillation: Concept and an application. Bull Amer Meteor Soc 68: 1218–1225

Maheras P, Kutiel H (1999) Spatial and temporal variations in the temperature regime in the Mediterranean and their relationship with circulation during the last century. Int J Climatol 19: 745–764

Maheras P, Kutiel H, Kolyva-Machera F (1997) Evolution de la pression atmospherique en Europe meridionale et en Mediterranée durant la dérnier période séculaire. Pub Assoc Int Climatol 10: 304–312

Maheras P, Kutiel H, Vafiadis M (1998) Tendances spatiales et temporelles de la pression atmospherique de surface et des geopotentiels de 500 hPa en Europe meridionale et en Mediterranée durant la période 1950–1994. Pub Assoc Int Climatol 11: 345–351

Maheras P, Xoplaki E, Kutiel H (1999) Wet and dry monthly anomalies across the Mediterranean basin and their relationship with circulation 1860–1990. Theor Appl Climatol 64: 189–199

Rogers JC (1984) The association between the north Atlantic oscillation and the southern oscillation in the northern hemisphere. Mon Wea Rev 112: 1999–2015

Rogers JC (1990) Patterns of low-frequency monthly sea level pressure variability (1899–1986) and associated wave cyclone frequencies. J Climate 3: 1364–1379

Rogers JC, van Loon H (1979) The seasaw in winter temperatures between Greenland and northern Europe. Part II: Some oceanic and atmospheric effects in middle and high altitudes. Mon Wea Rev 107: 1364–1379

Stephenson DB, Pavan V, Bojariu R (2000) Is the north Atlantic oscillation a random walk? Int J Climatol 20: 1–18

van Loon H, Rogers JC (1978) The seasaw in winter temperatures between Greenland and northern Europe. Part I: General description. Mon Wea Rev 106: 296–310

Wallace J, Gutzler D (1981) Teleconnections in the geopotential height field during the Northern Hemisphere winter. Mon Wea Rev 109: 784–812

Yin ZY (1999) Winter temperature anomalies of the north China plain and macroscale extratropical circulation patterns. Int J Climatol 19: 291–308

Authors' addresses: H. Kutiel (kutiel@geo.haifa.ac.il), Department of Geography, University of Haifa, Haifa 31905, Israel and Y. Benaroch (y_benaroch@yahoo.com), Department of Geography, University of Haifa, Haifa 31905, Israel and Israel Meteorological Service, Bet-Dagan 50250, Israel.